



Trans. Nonferrous Met. Soc. China 27(2017) 1656-1664

Transactions of Nonferrous Metals Society of China

www.tnmsc.cn



Effects of additives on zinc electrodeposition from alkaline zincate solution

Liang YUAN¹, Zhi-ying DING¹, Shi-jun LIU¹, Wei-fa SHU², Ya-ning HE¹

1. School of Chemistry and Chemical Engineering, Central South University, Changsha 410083, China; 2. 8511 Research Institute of China Aerospace Science & Industry Group, Nanjing 210017, China

Received 13 June 2016; accepted 23 February 2017

Abstract: The effects of additives on the surface and cross-sectional morphologies of zinc deposits on iron substrate from alkaline zincate solution were characterized by scanning electron microscope (SEM). The cathodic reaction mechanisms under various concentrations of additives were investigated using cyclic voltammetry (CV) and electrochemical impedance spectroscopy (EIS) techniques. It is found that with increasing the additive A content in the bath solution, the nucleation overpotential (NOP) value is obviously increased and the inhibition effect is strengthened. This may be mainly due to the adsorption of additive A on the cathodic electrode surface, which can cover the active sites and block the discharge reduction. The results of EIS analysis indicate that the rate-determining step of zinc electrodeposition process is changed from mixed control step into electrochemical reduction step in the presence of additive A. However, any quantity of additive B has little effect on the NOP value and the inhibition effect is not obvious. Furthermore, addition of additive A and additive B at the same time displays the strongest inhibition effect and shows a strong synergism because of their co-adsorption on the cathodic electrode surface.

Key words: electrodeposition; zinc; additives; alkaline zincate solution; morphology

1 Introduction

Zinc coating plays an indispensable contribution in protecting steel from corrosion due to its excellent anticorrosive properties by the formation of passive layer in contact with air and is widely used in more and more fields [1-5]. It can be obtained by electrolysis from a diversity of simple or complex bath, generally including cyanide and cyanide-free zinc plating baths. It is well known that traditional alkaline cyanide-based zinc plating is broadly employed in aerospace field for its stable bath performance, good coating quality and fine grains [6]. However, It is restricted gradually since cyanide is highly toxic and highly contaminated [7]. Recently, many researches about zinc electroplating in cyanide-free baths have been carried out, such as potassium chloride solution [8], sulfate solution [9–11], alkaline zincate solution [5,12] and ammonia containing solution [13,14]. Among numerous zinc electroplating baths, alkaline zincate solution gains a wider range of application due to its advantages of simple bath composition, good dispersion and favorable coverage capacity. It is likely that alkaline cyanide will be replaced by the alkaline zincate solution to be applied in aerospace fields.

For alkaline zincate electroplating solution, it is necessary to introduce suitable additives to control the deposition quality and performance. Organic additives can not only change the over-potential of electrode reaction, but also affect the preferred orientation and deposit morphology [15-20]. ZUNIGA et al [21] found that adding a given mass of quaternary aliphatic polyamine (QAA) into zinc planting bath in an alkaline non-cyanide medium led to a decrease in exchange current density, a change in crystal orientation and a decrease in grain size. PUSHPAVANAM [22] confirmed that polyvinyl alcohol had the function of making thickness distribution uniform and grain refining for non-cyanide alkaline zinc electrodeposition. PENG and WANG [12] measured the kinetic parameters of the electrode reactions during zinc electrodeposition in alkaline zincate solution. Most of the previous studies on alkaline zincate electrodeposition are mainly focused on the additive selection and deposition process. However, very little research is available to articulate

DOI: 10.1016/S1003-6326(17)60188-2

electrochemical behavior and mechanism analysis of additives, which perform profound effects on the metal crystal structure and coating properties.

In this work, cyclic voltammetry (CV) and electrochemical impedance spectroscopy (EIS) techniques were used to study the effects of additives on the zinc electrochemical deposition behaviors in alkaline zincate electrolyte, which was helpful for understanding the function and mechanism of additive. SEM was employed to characterize the difference of the surface and cross-sectional morphologies of the zinc coatings under the condition of different additives or combined additives.

2 Experimental

The electrolyte used for zinc electrodeposition was freshly prepared by dissolution of analytical pure regents in deionized water. The base electrolyte used in test was composed of 0.2 mol/L ZnO and 3.75 mol/L NaOH. Small scale electrolysis was performed in a plexiglass cell equipped with one vertical planar iron sheet used as cathode between two parallel lead plates used as anodes. The inter-electrode gap was 3 cm. The electrodeposition experiments were carried out at 30 °C under the cathodic current density of 2.5 A/dm² for 15 min. The surface and cross-sectional morphologies of freshly prepared deposits were characterized by a scanning electron microscope (SEM), using a PHILIPS XL 20 SE microscope. The additives used in test were a kind of quaternary ammonium salt (additive A) and a sulfonated salt of nicotinic acid (additive B). Both additives A and B were provided by the company.

Cyclic voltammetry and electrochemical impedance spectroscopy tests were carried out in a conventional three-electrode cell equipment using the CHI660C electrochemical analyzer. The working electrode was a glassy carbon electrode with diameter of 3 mm. Platinum plate with sizes of 10 mm × 10 mm was used as auxiliary electrode. The saturated calomel electrode (SCE), mounted inside a Luggin capillary, was used as a reference electrode and all potentials were referred to this electrode. All tests were conducted at 25 °C. Before each electrochemical measurement, the electrodes were mechanically polished to a mirror with successively finer grades of emery paper and 0.5 µm Al₂O₃ powder, then cleaned with alcohol ultrasonic and demonized water ultrasonic for 2 min, respectively. High purity nitrogen was used to sparge out dissolved oxygen for 15 min prior to each electrochemical experiment. All cyclic voltammograms were performed at a scan rate of 10 mV/s. For the EIS tests, the working electrode was immersed in the base solution for 10 min to ensure on a static condition. The scanning frequency range was 10 mHz-100 kHz with a amplitude of 5 mV.

3 Results and discussion

3.1 Deposit morphology

The additives play the most important role in forming compact and smooth zinc deposits from alkaline zincate solution. The surface and cross-sectional morphologies of zinc deposits are presented in Fig. 1. It is clearly seen that zinc deposit obtained from bath solution shows large irregular grains and obvious grain boundaries as presented in Fig. 1(a). In the base solution with additive B, little has changed on the morphology of zinc deposit (Fig. 1(b)), where large irregular grains are also clearly observed. Figure 1(b₁) shows that the adhesion strength between the deposit and substrate is poor as well as that in Fig. 1(a₁). The large irregular grains result in poor adhesion strength. However, in the case of a given quantity of additive A, the zinc deposit is compact and the grains are much smaller, no grain boundaries appear as shown in Fig. 1(c). The changes in the deposit morphology are attributed to the adsorption of additive A to block the growth centers of zinc and retain the discharge reduction on the cathode, which indicate that additive A plays a role of grain refining. It is obvious from Fig. 1(d) that a smooth, bright and uniform deposit is formed when both additives A and B are added in the base solution. This is thought to be the synergism of the combined additives on the surface morphology. The results of the fine surface quality may be attributed to the effective adsorption of additive A on the cathodic surface firstly, then additive B is adsorbed on the recess of the absorbed layer, thus, a much tight adsorption layer is formed because of their synergism. It is also evident that additive B has the function of leveling ability.

3.2 Voltammetric study in the presence of additives

The cathodic parts of cyclic voltammetry curves in the base solution and additive-containing solutions are illustrated in Fig. 2. A crossover appears between the cathodic and anodic parts of the curves, which indicates that nucleation is involved in the zinc electrodeposition process [4,23]. In Fig. 2(a), the region BDE is called as a nucleation hysteresis loop and characterized by several important features. Such hysteresis loops are also observed in Figs. 1(b)-(d), where the concentration of additive A impacts the shape of hysteresis loops significantly. The potential difference between the nucleation potential $(\varphi_{nu}, point B)$ and the crossover potential $(\varphi_{co}, point E)$ is defined as nucleation overpotential (NOP), which is regarded as a yardstick of cathode polarization. Higher NOP value implies stronger polarization.

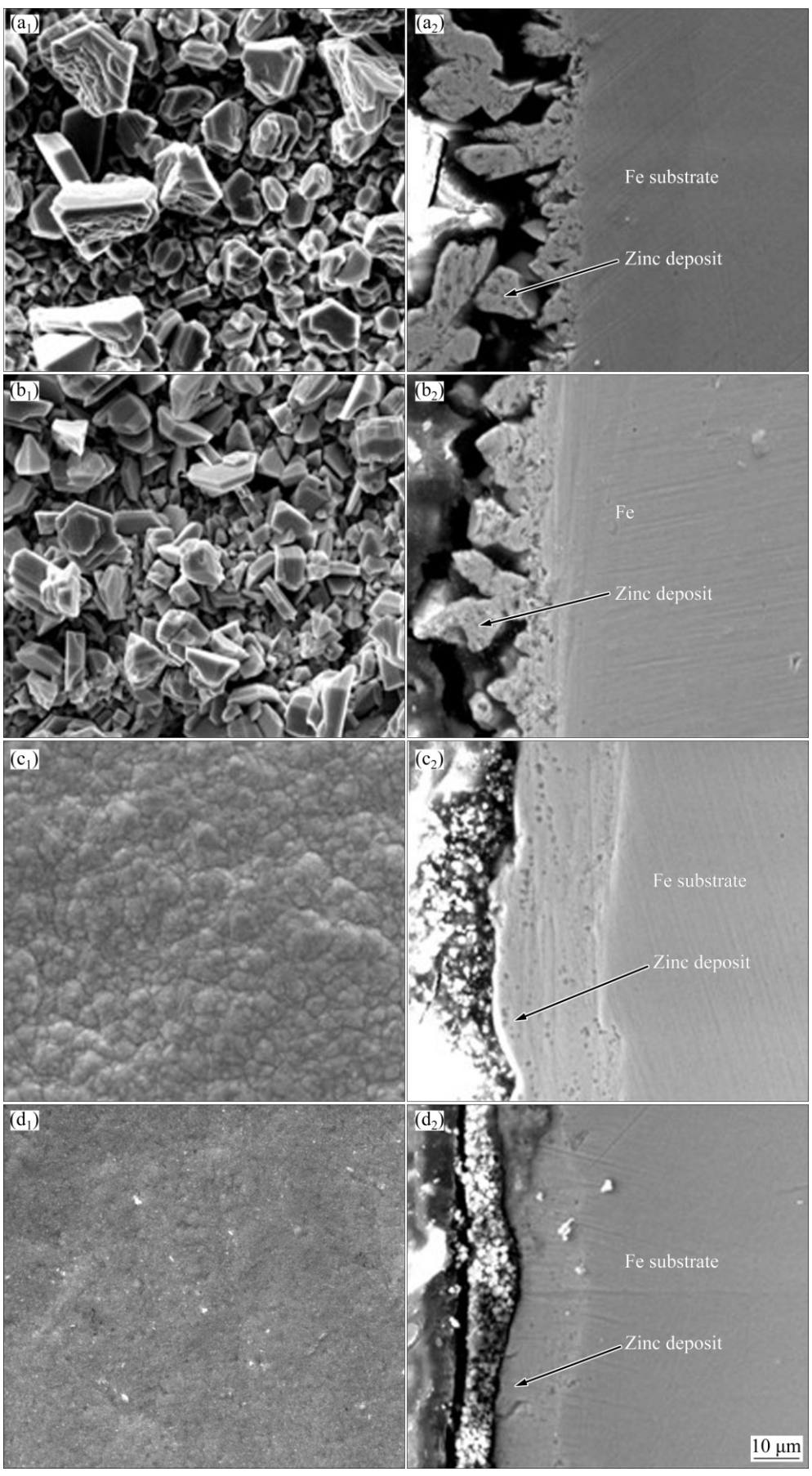


Fig. 1 Surface and cross-sectional SEM images of zinc deposits on iron substrate from alkaline zincate solution: (a_1, a_2) Base solution; (b_1, b_2) With 1 mL/L additive B; (c_1, c_2) With 16 mL/L additive A; (d_1, d_2) With 16 mL/L additive A and 1 mL/L additive B

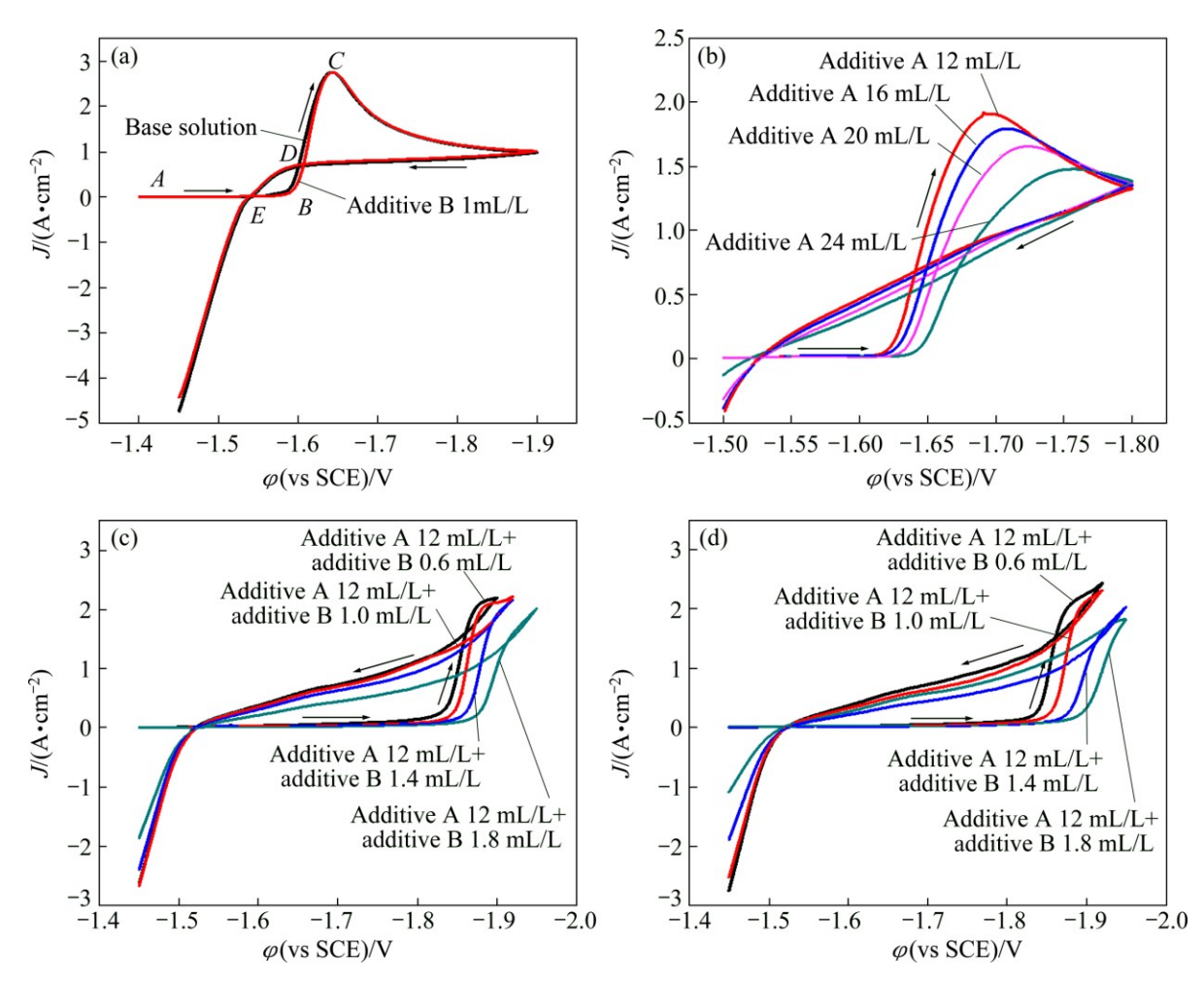


Fig. 2 Cathodic part of cyclic voltammograms for zinc deposition from alkaline zincate solution: (a) With additive B; (b) With additive A; (c, d) With combined additives

The NOP values of zinc electrodeposition in alkaline zincate solutions obtained from Fig. 2 are listed in Table 1. It is obvious that with increasing the additive A content in the bath solution, the NOP values progressively increase. In Table 1, the NOP value increases to 94 mV by adding 12 mL/L additive A. Compared with the base solution, the NOP value increases by 24 mV. The results reveal that the additive A has an inhibition effect on zinc electrodeposition of cathodic process. This effect is enhanced along with the concentration of additive A. By contrast, the inhibition effect of additive B is not obvious. The NOP value is increased by only 1 mV when 1.0 mL/L additive B is added in the base solution. By adding the combined additives, the inhibition effect is stronger than that when the two additives are added separately. For example, the NOP value is 326 mV when 12 mL/L additive A and 1.0 mL/L additive B are added in the base solution, which is far greater than that of additives presented separately. Accordingly, there is a strong synergism between additive A and additive B.

Table 1 Effects of additives on nucleation overpotential values for zinc electrodeposition from alkaline zincate solution

Concentration	on/(mL·L $^{-1}$)	- / X 7	/ \$7	NOD/mV	
Additive A	Additive B	$-\varphi_{\rm co}/{\rm mV}$	$-\varphi_{ m nu}/{ m mV}$	-NOP/mV	
0	0	1528	1598	70	
0	1.0	1528	1599	71	
12	0	1528	1622	94	
16	0	1528	1630	102	
20	0	1528	1638	110	
24	0	1528	1644	116	
12	0.6	1522	1829	307	
12	1.0	1522	1848	326	
12	1.4	1521	1861	340	
12	1.8	1524	1875	351	
16	0.6	1522	1838	316	
16	1.0	1521	1854	333	
16	1.4	1520	1872	352	
16	1.8	1521	1889	368	

The synergism can be attributed to the adsorption of additives on the surface of cathodic electrode [24,25]. When additive A is added in the electrolyte, its adsorption results in the formation of a compact adsorption layer to block the active nucleation sites on the cathodic surface and inhibit the discharge reaction of zinc ion. It can be reflected from the increase trend of the NOP values. At higher concentration of additive A, with the enhancement of the blocking effect on the active sites, a higher driving force for zinc ion reduction will be required. When additive B is added in base solution, little effective adsorption layer on the cathodic electrode surface is formed. Therefore, the inhibition on the zinc electrodeposition is not obvious. With the combined additives, the co-adsorption of additive A and additive B on the cathodic electrode surface is likely to form a stronger synergism, which strengthens the inhibition further.

3.3 Impedance spectra study in the presence of additives

The Nyquist plots of EIS tests at base solution and different concentrations of additive A are shown in Fig. 3, where the additive A has a significant effect on the EIS spectra. The diagram for the base solution is composed of a capacitive loop approximate semicircle in high frequency range and a sloping line in low frequency

range (Fig. 3(a)). It is believed that high frequency capacitive loop is attributed to the double layer capacitance and charge transfer resistance. For the low frequency region, it is characterized by a typical Warburg impedance (the sloping line) and related to the diffusion of zinc complex ion in the bulk solution. The EIS analysis indicates that zinc electrodeposition process is controlled by charge transfer in high frequency and zinc complex ion diffusion in low frequency due to the difference of charge discharge relaxation and diffusion relaxation. Both electrochemical polarization and concentration polarization are accompanied by the whole cathodic reduction process [26,27]. From Fig. 3(b), it is clear that additive A significantly affects the high and low frequency loops. The Nyquist impedance diagrams are composed of two capacitive loops and two inductive loops, which indicates that zinc electrodeposition process in additive A-containing solution is only controlled by discharge reduction reaction of zinc complex ion [28]. It can be concluded that additive A changes the rate-determining and influences step the zinc electrodeposition behavior, the rate-determining step is changed from mixed control step to discharge reduction step of zinc complex ion.

Fitting procedure is applied using commercial Zview software and the equivalent circuits are depicted in Fig. 4, which shows the equivalent circuits of

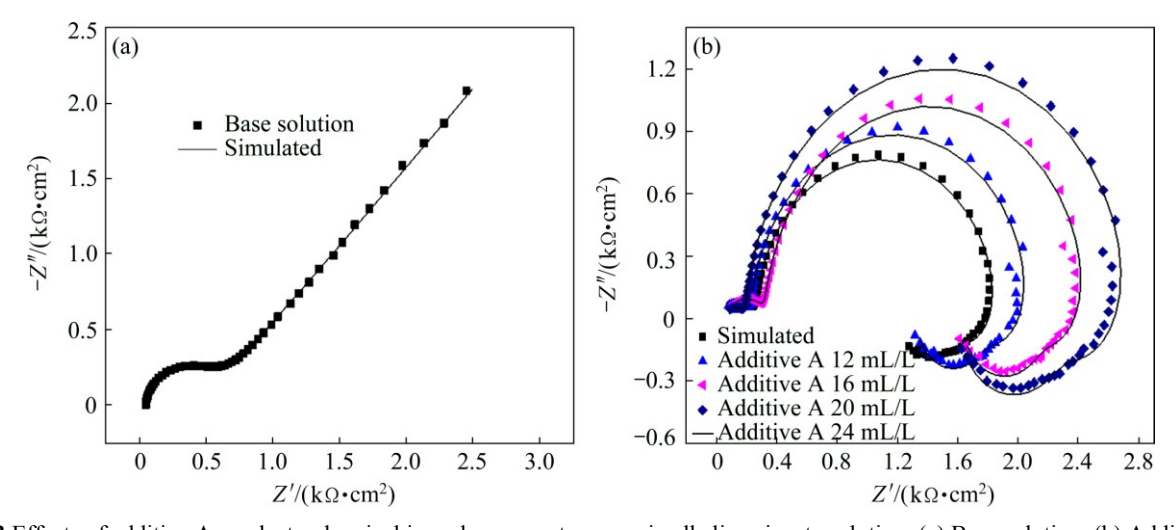


Fig. 3 Effects of additive A on electrochemical impedance spectroscopy in alkaline zincate solution: (a) Base solution; (b) Additive A content solution

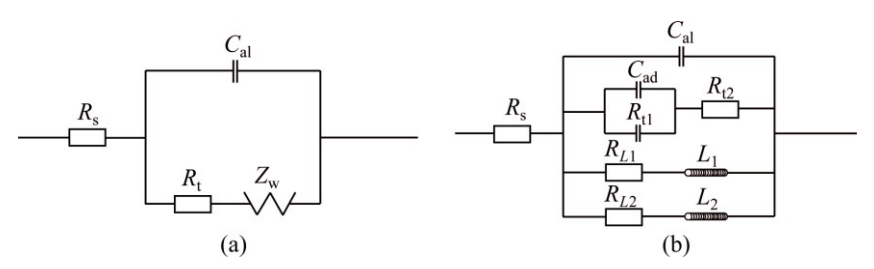


Fig. 4 Corresponding equivalent circuit for zinc electrodeposition in alkaline zincate solution: (a) Equivalent circuit for Figs. 3(a) and Figs. 5; (b) Equivalent circuit for Figs. 3(b) and Figs. 6(a) and (b)

Figs. 3(a) and (b), respectively. In Fig. 4(a), R_s , R_t , C_{dl} , and Z_w are the solution resistance, the charge transfer resistance, the double layer capacitance, and Warburg impedance, respectively. The smaller the value of R_t is, the easier the electrode discharge reduction reacts. The capacitance in the circuit is supported by parameter n. This parameter describes the width of the relaxation time in the frequency space, which is related to the constant phase element (CPE) used to fit the data. The values of n_1 and n_2 are deviated from 1 and 0.5, respectively, which indicate that there is a dispersion effect between the double layer capacitor $C_{\rm dl}$ and the Warburg. In Fig. 4(b), R_s is the solution resistance; R_{t1} is the charge transfer resistance of the first discharge reduction reaction; C_{dl} is the double layer capacity; C_{ad} is the capacity caused by electrochemistry active middle product of Zn(OH)_{ad} adsorbed on the cathodic surface; R_{t2} is the charge transfer resistance of the second discharge reduction reaction; R_{L1} and R_{L2} are Faraday resistance; L_1 and L_2 are inductance caused by free zinc atoms and additives adsorbed on the cathodic surface. Solid lines in Fig. 3 are the typical fitted curves. Table 2 and Table 3 list the corresponding values of elements used in equivalent circuits. It is clear that the value of $R_{\rm tl}$ in 16 mL/L additive A-containing solution is 5 times more than that in base solution, which indicates that the inhibition effect of additive A on the zinc discharge reaction is obvious.

The Nyquist impedance diagrams of zinc electrodeposition from the base solution and additive B-

 Table 2
 Parameters of equivalent circuit for zinc

 electrodeposition from base solution

$R_{\rm s}/(\Omega\cdot{\rm cm}^2)$	$C_{\rm dl}/({\rm mF\cdot cm^2})$	n_1	$R_t/(\Omega \cdot \mathrm{cm}^2)$	n_2
52.79	46.3	0.9336	567	0.4872

containing solution are shown in Fig. 5, where the typical Warburg impedance spectra are displayed. It can be concluded through the EIS spectra analysis that zinc electrodeposition process in additive B-containing solution is still controlled by charge transfer in high frequency and zinc complex ion diffusion in low frequency. The equivalent circuit of Fig. 4(a) is also used to fit the EIS curves in Fig. 5. The corresponding parameters of equivalent circuit are listed in Table 4. It is clear that R_t value increases slowly with the concentration of additive B, which indicates that the inhibition effect of additive B is limited.

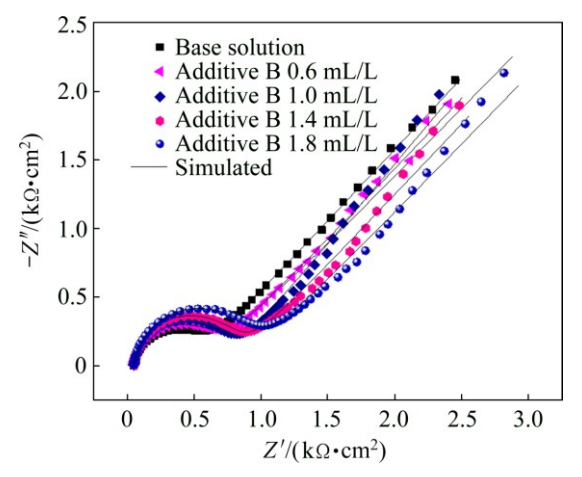


Fig. 5 Effects of additive B on electrochemical impedance spectroscopy in alkaline zincate solution

The Nyquist plots of EIS tests under the condition of additive A and additive B are presented in Fig. 6. The shapes of the Nyquist impedance diagrams are all similar and composed of two capacitive loops and two inductive loops as shown in Fig. 3(b). This indicates that zinc electrodeposition process is also controlled by discharge

Table 3 Parameters of equivalent circuit for zinc electrodeposition from additive A-containing solution

Concentration of additive A/($mL \cdot L^{-1}$)	$C_{\rm dl}/$ $({ m mF}\cdot{ m cm}^2)$	n_1	$R_{\rm tl}/$ $(\Omega \cdot {\rm cm}^2)$	$C_{\rm ad}$ / (mF·cm ²)	n_2	$R_{t2}/$ $(\Omega \cdot \text{cm}^2)$	$R_{\rm L1}/$ $(\Omega \cdot {\rm cm}^2)$	$L_1/$ (H·cm ²)	$R_{\rm L2}/$ $(\Omega \cdot {\rm cm}^2)$	$L_2/$ (H·cm ²)
12	1240	0.9423	3780	22.7	0.4883	243	7155	8857	1688	977
16	610	0.9311	3159	28.2	0.5021	300	6531	7382	14999	893
20	830	0.9300	2467	38.9	0.5113	358	14829	1053	7520	9472
24	940	0.9344	3558	32.4	0.4791	424	19852	1205	8914	10649

Table 4 Parameters of equivalent circuit for zinc electrodeposition from additive B-containing solution

				8		
Concentration of additive $B/(mL \cdot L^{-1})$	$R_{\rm s}/(\Omega\cdot{\rm cm}^2)$	$C_{\rm dl}/({\rm mF\cdot cm}^2)$	n_1	$R_t/(\Omega \cdot \text{cm}^2)$	n_2	
0	52.79	46.3	0.9336	567	0.4872	
0.6	48.72	45.6	0.9309	594	0.5158	
1.0	51.48	32.1	0.9290	692	0.5205	
1.4	51.65	24.7	0.9374	730	0.4791	
1.8	51.92	22.6	0.9355	841	0.4809	

reduction reaction of zinc complex ion. Such patterns in impedance spectra can also be simply explained by equivalent circuit shown in Fig. 4(b). The parameters of equivalent circuit are listed in Table 5 and Table 6. It is apparent that the value of $R_{\rm t}$ is much greater than that when additives are added separately. The results of synergism between additives A and B are in close agreement with the cyclic voltammetry.

During the zinc electrodeposition process from additive A-containing solution or combined additives-containing solution, a layer is formed due to the adsorption on the cathodic surface, where the active sites on the cathode are covered by the adsorption layer. The reduction reaction of zinc complex ion is limited on the cathodic surface. Then, the zinc complex ion just can participate in the discharge reaction only on the unoccupied active sites. Thus, the discharge reduction reaction step of zinc complex ion turns into the

rate-determining step. However, there is no adsorption layer on the cathode surface in the base solution or additive B-containing solution, zinc complex ion can participate in reaction on the uncovered cathodic surface easily and zinc electrodeposition process is controlled by the mixed diffusion and charge transfer of zinc complex ion.

4 Conclusions

- 1) The surface morphology of zinc deposits varies significantly with the addition of additives. The additive A and additive B play a role of grain refining and surface leveling respectively, which results in smooth, bright and uniform deposits.
- 2) Zinc electrodeposition process is inhibited in the presence of additive A due to enhancement in coverage on the cathodic surface, where the discharge reduction

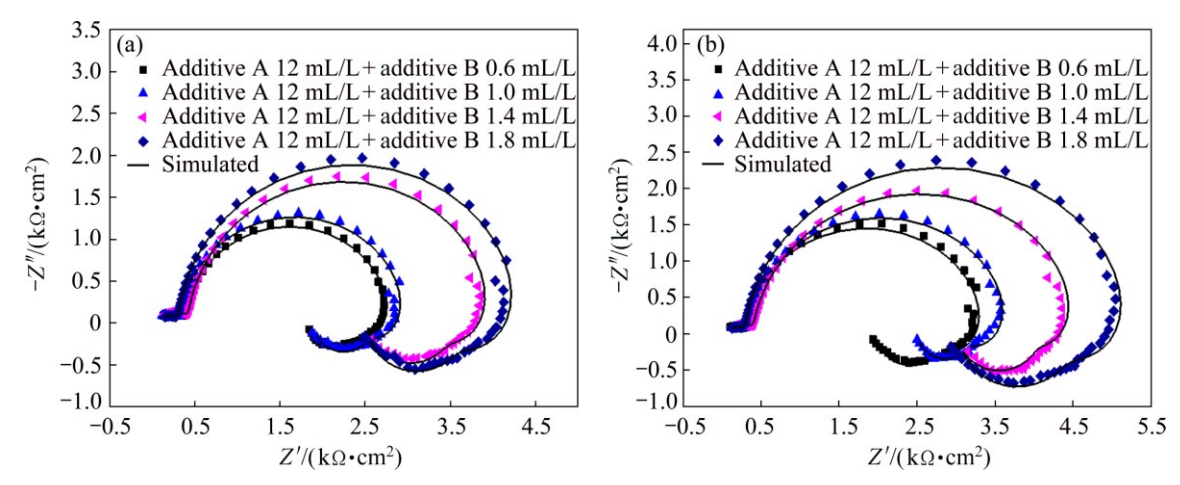


Fig. 6 Electrochemical impedance spectroscopy in combined additives content alkaline zincate solution: (a) 12 mL/L additive A and different amount of additive B; (b) 16 mL/L additive A and different amount of additive B

Table 5 Parameters of equivalent circuit of Fig. 6(a) during zinc electrodeposition in combined additives content solution (12 mL/L additive A)

Concentration of	$C_{ m dl}$	n_1	$R_{\rm tl}$	$C_{ m ad}$ /	n_2	R_{t2}	$R_{\rm L1}$	L_1	$R_{\rm L2}$	L_2 /
additive B/(mL·L ⁻¹)	(mF·cm ²)	1	$(\Omega \cdot \text{cm}^2)$	(mF·cm ²)		$(\Omega \cdot cm^2)$	$(\Omega \cdot cm^2)$	(H·cm ²)	$(\Omega \cdot cm^2)$	(H·cm ²)
0.6	12.3	0.9320	3780	22.7	0.4875	243	7155	8857	16880	977
1.0	14.0	0.9309	3837	34.9	0.5158	268	10756	1128	17376	16994
1.4	6.1	0.9259	4059	28.2	0.5205	300	6531	7382	14999	893
1.8	10.1	0.9311	4210	18.2	0.4791	312	26276	1819	9421	15649

Table 6 Parameters of equivalent circuit of Fig. 6(b) during zinc electrodeposition in combined additives content solution (16 mL/L additive A)

Concentration of	$C_{\rm dl}$ /	n_1	$R_{\rm tl}$	C_{ad}	n_2	R_{t2}	$R_{\rm L1}$	L_1 /	$R_{\rm L2}$	L_2 /
additive B/(mL·L ⁻¹)	(mF·cm ²)	**1	$(\Omega \cdot cm^2)$	(mF·cm ²)		$(\Omega \cdot cm^2)$	$(\Omega \cdot cm^2)$	(H·cm ²)	$(\Omega \cdot \text{cm}^2)$	(H·cm ²)
0.6	10.8	0.9311	3920	18.3	0.4800	267	24804	1683	9200	14800
1.0	6.8	0.9324	4138	35.7	0.5114	314	14857	809	7189	7609
1.4	8.3	0.9265	4267	38.9	0.5111	358	14829	1053	7520	9472
1.8	9.5	0.9344	4354	29.4	0.4700	380	27238	1764	11644	23092

reaction of zinc complex ion is found to be the ratecontrolling step.

- 3) For additive B, there is no adsorbed layer formed on the cathodic electrode surface, and the inhibition effect is not obvious, where the rate-determining step is controlled by the mixture of zinc complex ion diffusion and charge transfer.
- 4) When the combined additives are added in the base solution, there is a strong synergistic effect, which displays the strongest inhibition in zinc complex ion discharge reduction due to their co-adsorption on the cathodic electrode surface. The rate-determining step is also changed to discharge reduction reaction.

References

- MOUANGA M, RICQ L, DOUGLADE G. Influence of coumarin on zinc electrodeposition [J]. Surface and Coatings Technology, 2006, 201(3): 762–767.
- [2] CARVALHO M F, BARBANO E P, CARLOS I A. Influence of disodium ethylenediaminetetraacetate on zinc electrodeposition process and on the morphology, chemical composition and structure of the electrodeposits [J]. Electrochimica Acta, 2013, 109: 798–808.
- [3] GREUL T, GERDENITSCH J, HASSEL A W. The influence of tin ions on the electrodeposition of zinc [J]. Materials and Corrosion, 2014, 65(4): 410–415.
- [4] OLIVEIRA E M, CARLOS I A. Voltammetric and morphological characterization of zinc electrodeposition from acid electrolytes containing boric-polyalcohol complexes [J]. Journal of Applied Electrochemistry, 2008, 38(9): 1203–1210.
- [5] CARVALHO M F, CARLOS I A. Zinc electrodeposition from alkaline solution containing trisodium nitrilotriacetic added [J]. Electrochimica Acta, 2013, 113: 229–239.
- [6] HOYER P, RUSHMERE J. Alkaline cyanide zinc electroplating: US patent, 3734839 [P]. 1973–05–22.
- [7] REN Feng-zhang, YIN Li-tao, WANG Shan-shan. Cyanide-free silver electroplating process in thiosulfate bath and microstructure analysis of Ag coatings [J]. Transactions of Nonferrous Metals Society of China, 2013, 23(12): 3822–3828.
- [8] SINGH D N, DEY M, SINGH V. Role of buffering and complexing agents in zinc plating chloride baths on corrosion resistance of produced coatings [J]. Corrosion, 2002, 58(11): 971–980.
- [9] ZHANG Qi-bo, HUA Yi-xin. Effects of temperature and current density on zinc electrodeposition from acidic sulfate electrolyte with [BMIM]HSO₄ as additive [J]. Journal of Applied Electrochemistry, 2009, 39(8): 1207–1216.
- [10] LI Mou-cheng, LUO Su-zhen, QIAN Yu-hai. Effect of additives on electrodeposition of nanocrystalline zinc from acidic sulfate solutions [J]. Journal of The Electrochemical Society, 2007, 154(11): D567–D571.
- [11] SAJJADNEJAD M, MOZAFARI A, OMIDVAR H. Preparation and corrosion resistance of pulse electrodeposited Zn and Zn-SiC nanocomposite coatings [J]. Applied Surface Science, 2014, 300: 1-7.

- [12] PENG Wen-jie, WANG Yun-yan. Kinetics of Zn cathodic deposition in alkaline zincate solution [J]. Journal of Central South University of Technology, 2006, 13: 637–641.
- [13] XIA Zhi-mei, YANG Sheng-hai, DUAN Liang-hong. Effects of Br⁻ and Γ concentrations on Zn electrodeposition from ammoniacal electrolytes [J]. International Journal of Minerals, Metallurgy and Materials, 2015, 22(7): 682–687.
- [14] GOMES A, SILVA-PEREIRA M I. Pulsed electrodeposition of Zn in the presence of surfactants [J]. Electrochimica Acta, 2006, 51(7): 1342–1350.
- [15] SONG K D, KIM K B, HAN S H. Effect of additives on hydrogen evolution and absorption during Zn electrodeposition investigated by EQCM [J]. Electrochemical and Solid State Letters, 2004, 7(2): 20–24.
- [16] LEE J Y, KIM J W, LEE M K. Effects of organic additives on initial stages of zinc electroplating on iron [J]. Journal of The Electrochemical Society, 2004, 151(1): C25–C31.
- [17] NAKANO H, FUKUSHIMA H. Morphology control of zinc deposits of electrogalvanized steel sheets [J]. Journal of the Iron and Steel Institute of Japan, 2002, 88(5): 236–242.
- [18] KAVITHA B, SANTHOSH P, RENUKADEVI M. Role of organic additives on zinc plating [J]. Surface and Coatings Technology, 2006, 201(6): 3438–3442.
- [19] NAYANA K O, VENKATESHA T V, PRAVEEN B M. Synergistic effect of additives on bright nanocrystalline zinc electrodeposition [J]. Journal of Applied Electrochemistry, 2011, 41(1): 39–49.
- [20] BALLESTEROS J C, DÍAZ-ARISTA P, MEAS Y. Zinc electrodeposition in the presence of polyethylene glycol 20000 [J]. Electrochimica Acta, 2007, 52(11): 3686–3696.
- [21] ZUNIGA V, ORTEGA R, MEAS Y. Electrodeposition of zinc from an alkaline non-cyanide bath: Influence of a quaternary aliphatic polyamine [J]. Plating and Surface Finishing, 2004, 91(6): 46–51.
- [22] PUSHPAVANAM M. Role of additives in bright zinc deposition from cyanide free alkaline baths[J]. Journal of Applied Electrochemistry, 2006, 36(3): 315–322.
- [23] WEI Liu, YANG Tian-zu, ZHOU Qiong-hua. Electrodeposition of Sb(III) in alkaline solutions containing xylitol [J]. Transactions of Nonferrous Metals Society of China, 2012, 22(4): 949–957.
- [24] LEHR I L, SAIDMAN S B. Influence of sodium bis(2-ethylhexyl) sulfosuccinate (AOT) on zinc electrodeposition [J]. Applied Surface Science, 2012, 258(10): 4417–4423.
- [25] AABOUBI O, DOUGLADE J, ABENAQUI X. Influence of tartaric acid on zinc electrodeposition from sulphate bath [J]. Electrochimica Acta, 2011, 56(23): 7885–7889.
- [26] DAROWICKI K, SLEPSKI P, SZOCINSKI M. Application of the dynamic EIS to investigation of transport within organic coatings [J]. Progress in Organic Coatings, 2005, 52(4): 306–310.
- [27] LONG Jin-ming, ZHANG Zha, GUO Zhong-cheng. Electrochemical study of the additive-effect on Sn electrodeposition in a methansulfonate acid electrolyte [J]. Advanced Materials Research, 2012, 460: 7–10.
- [28] PENG Wen-jie, WANG Yun-yan. Mechanism of zinc electroplating in alkaline zincate solution [J]. Journal of Central South University of Technology, 2007, 14: 37–41.

添加剂对碱性锌酸盐溶液锌电沉积的影响

袁 亮1, 丁治英1, 刘士军1, 舒伟发2, 何亚宁1

- 1. 中南大学 化学与化工学院,长沙 410083;
- 2. 中国航天科技集团 8511 研究所,南京 210017

摘 要:采用扫描电镜表征添加剂对碱性锌酸盐溶液锌电沉积层表面和截面形貌的影响。运用循环伏安法和交流阻抗技术研究不同浓度添加剂在锌电沉积过程中的作用机理。研究结果表明,随着添加剂 A 浓度的增加,锌的形核过电位增大,对锌还原的抑制作用增强。这是由于添加剂 A 在阴极表面的吸附作用覆盖了阴极表面活性位点,并阻碍了阴极放电造成的。交流阻抗谱分析表明,在添加剂 A 存在的情况下,锌电沉积的控制步骤由扩散控制变为混合控制。添加剂 B 对锌的形核过电位值的影响较小,抑制效果不明显,但同时加入两种添加剂时,在电极表面的吸附作用更加显著,对锌电沉积的抑制作用最大,两者表现出明显的协同作用。

关键词: 电沉积; 锌; 添加剂; 碱性锌酸盐溶液; 形貌

(Edited by Xiang-qun LI)